



The Thomas Jefferson National Accelerator Facility
Theory Group Preprint Series

Additional copies are available from the authors.

The Southeastern Universities Research Association (SURA) operates the Thomas Jefferson National Accelerator Facility for the United States Department of Energy under contract DE-AC05-84ER40150.

DISCLAIMER

This report was prepared as an account of work sponsored by the United States government. Neither the United States nor the United States Department of Energy, nor any of their employees, makes any warranty, expressed or implied, or assumes any legal liability or responsibility for the accuracy, completeness, or usefulness of any information, apparatus, product, or process disclosed, or represents that its use would not infringe privately owned rights. Reference herein to any specific commercial product, process, or service by trade name, mark, manufacturer, or otherwise, does not necessarily constitute or imply its endorsement, recommendation, or favoring by the United States government or any agency thereof. The views and opinions of authors expressed herein do not necessarily state or reflect those of the United States government or any agency thereof.

SPIN STRUCTURE OF THE PROTON: a quark modeler's view

Nathan Isgur
Jefferson Lab

12000 Jefferson Avenue, Newport News, Virginia 23606

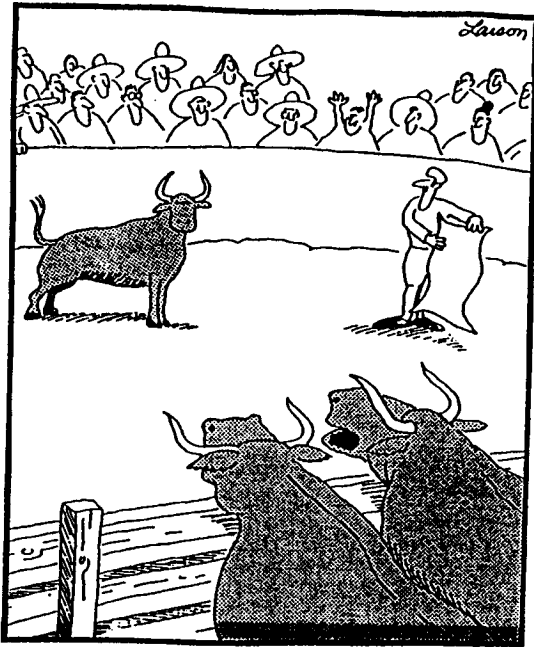
In these lectures I argue that our response to the spin crisis should not be to abandon the naïve quark model baby, but rather to allow it to mature. I begin by recalling what a beautiful baby the quark model is via an overview of its successes in spectroscopy, dynamics, and *valence* spin structure; I also introduce the conservative hypothesis that dynamical $q\bar{q}$ pairs are its key missing ingredient. I then discuss dressing the baby. I first show that it can be clothed in glue without changing its spectroscopic successes. In the process, several dynamical mysteries associated with quark model spectroscopy are potentially explained. Next I dress the baby in $q\bar{q}$ pairs, first showing that this can be done without compromising the naïve quark model's success with either spectroscopy or the OZI rule. Finally, I show that despite their near invisibility elsewhere, pairs do play an important role in the proton's spin structure by creating an antipolarized $q\bar{q}$ sea. In the context of an explicit calculation I demonstrate that it is plausible that the entire "spin crisis" arises from this effect.

1 Introductory Remarks

Sometimes, it seems to me, we get a little carried away with the beauty and precision of deep inelastic scattering as a probe of the quark-gluon structure of the proton. It is undeniably satisfying to be able to make rigorous statements about strongly interacting systems: it is such a rare experience. However, deep inelastic scattering can, *via* perturbative QCD, only tell us "what is there". It is thus only a prelude to understanding *via* Strong QCD¹ "why it is there".

There are those who would argue that it is sufficient to compare the results of experiments against lattice simulations of QCD. I certainly agree that this is our principal route toward precision tests of Strong QCD. However, I would argue that such comparisons cannot act as a substitute for *understanding* QCD, and that it would be a great failure of physics if we were to forfeit thinking about QCD to our computers.

QCD is undeniably very complex, so if we are to understand it, we will clearly have to find some way to simplify it. This is, of course, not new to QCD. Superconductivity is also intractable as a theory of 10^{23} crystalline nuclei and 10^{23} electrons, but it can be understood once the right low energy effective degrees of freedom - - - Cooper pairs and phonons - - - are identified. An example closer to home is nuclear physics: nuclear structure may be understood



"The Far Side" by Gary Larson is reprinted courtesy Chronicle Features, San Francisco, California. All rights reserved.

"Not the cape, Larry! Not the cape!"

Figure 1: The importance of knowing where to attack a problem.

very well in terms of the nucleonic low energy degrees of freedom interacting *via* few body effective potentials. Similarly, I believe that the central issue in Strong QCD is to identify the correct low energy degrees of freedom at the "quark model" scale $\mu_{QM} \sim 1$ GeV. In physics, as in many other callings, it is crucial to know where to attack a problem (see Fig. 1).

In these lectures I will argue that there are many good reasons to believe that the constituent quark model *is* a good starting point in this quest. When extended *via* the flux tube model, wherein the gluonic degrees of freedom are subsumed into flux tubes, the constituent quark model can be mapped onto QCD in the large N_c limit². After reviewing these matters, I will argue that,

while adequate for many purposes, this quark model must be further extended by "unquenching" (a $1/N_c$ effect) if it is to provide a satisfactory qualitative picture of Strong QCD. That is, I suggest that dynamical $q\bar{q}$ pairs are the key missing ingredient of the constituent quark model. In particular, I will show in an explicit model how one can "unquench" the quark model without spoiling its spectroscopic successes or ruining the OZI rule³. At the same time, we will see that while each light quark flavor may make a relatively small negative contribution to the net proton spin of order $1/N_c$, N_f such contributions can account for the observed "spin crisis".

2 Admiring the Baby

We begin with a quick overview of the successes of the constituent quark model. Given the subject of this meeting, I will focus on its successes in baryons. The two most important conclusions I expect you to draw from this overview are that:

- 1) The baryon spectrum behaves like a system consisting of three spin- $1/2$ degrees of freedom. In particular, there is no spectroscopic evidence for additional gluonic or $q\bar{q}$ degrees of freedom.
- 2) The low energy dynamics of the spectrum, including its static properties and photon and meson couplings, are consistent with the valence quarks carrying the spin of the proton.

2.1 Remembering Why We Love It: Spectroscopy

Figures 2-5 show the theoretical "evolution" of the spectroscopy of the first and second bands of excited states of the proton (corresponding to the low-lying negative parity states around 1600 MeV and the first band of positive parity excitations centered around 1950 MeV) in a popular constituent quark model⁴. Figure 2 shows these 28 states in the harmonic limit. In Figure 3 they are split up by the departure U of the central potential from harmonic form, *i.e.*, by the fact that the true potential is of Coulomb plus linear form. (Note that this effect immediately splits off two states with the quantum numbers of the ground state N and Δ by almost -400 MeV into the region of the negative parity excitations.) In Figure 4 these levels are further perturbed by hyperfine (spin-spin and tensor) interactions with a strength fixed by the observed ground state $\Delta - N$ splitting.

The experimental observations of these states are still today totally dominated by πN elastic partial wave analyses, so that states with weak πN couplings will have escaped detection. On the basis of a calculation⁵ of the

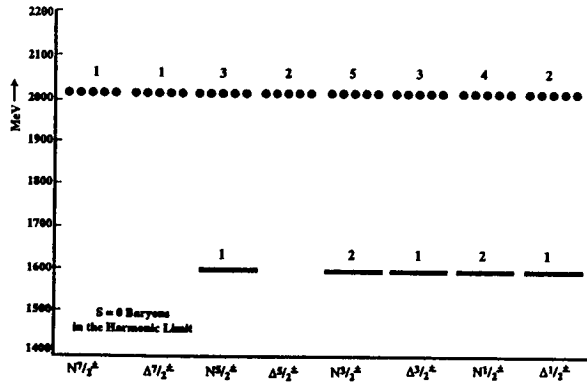


Figure 2: The first negative and positive parity bands of excited nucleons in the harmonic limit. Negative parity states are shown as solid bars; positive parity states as dotted bars.

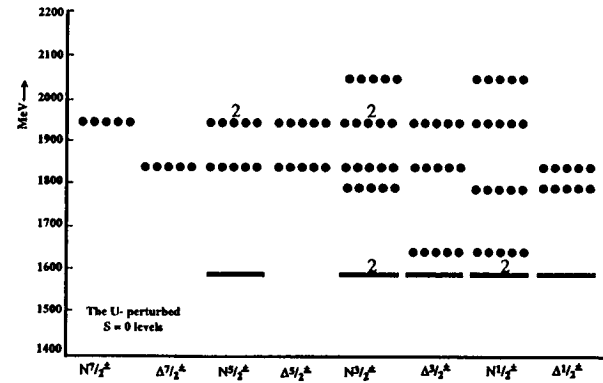


Figure 3: As in Fig. 2 with Coulomb plus linear confinement.

couplings of these states to the πN channel, one would expect experiments to have seen not 28 but rather just 17 states. Figure 5, in which the 11 weakly-coupled states (which all happen to be positive parity excitations) are marked by single dots while strongly-coupled states remain as in Fig. 4, shows that the actual situation is very close to what is expected from the naïve constituent quark model picture.

Perhaps the very good correspondence between the constituent quark model and experiment is an accident, but the simplest interpretation is that at low energy the proton behaves like a system with three spin-1/2 degrees of freedom. Moreover, these degrees of freedom do more than passively carry the proton's spin: they interact *via* spin-dependent forces which have important quantitative effects on the spectrum. In the next section we will see that these three spin-1/2 degrees of freedom also appear to determine the dynamics of these systems.

2.2 Remembering Why We Love It: Dynamics

Each of the observed states in Figure 5 has not only had its mass, spin, and parity determined, but also at least some of its dynamical properties. Table

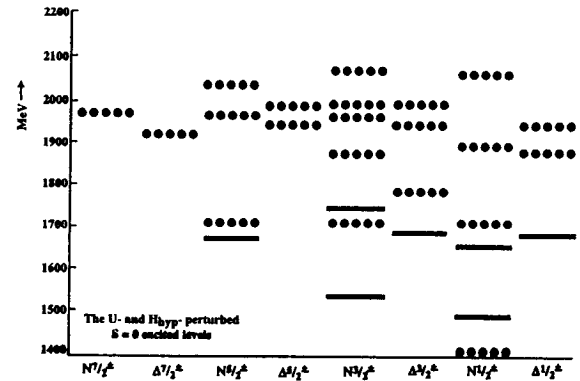


Figure 4: As in Fig. 3 with hyperfine interactions.

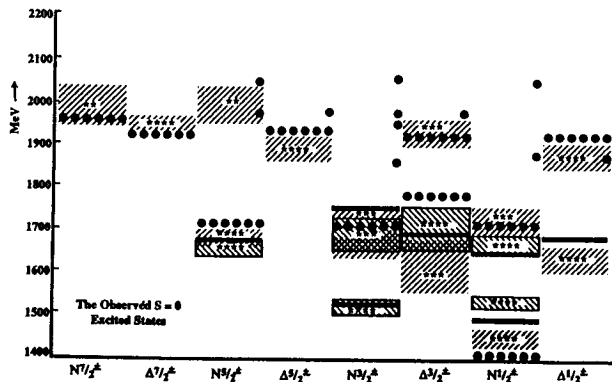


Figure 5: As in Fig. 4 with states weakly coupled to πN scattering now shown as single dots, and with the experimental masses shown as shaded regions. The shaded regions (with widths corresponding to the experimental uncertainty in the masses) are coded with the boxed negatively-sloped cross-hatching corresponding to negative parity states and the open positively-sloped cross-hatching corresponding to positive parity states.

1 shows just two of dozens of examples of the dynamical successes of the constituent quark model for baryons. These two states, the two lowest-lying $N^* \frac{1}{2}^-$ states, are especially interesting for a number of reasons. One is that they are predicted to be *very* strongly mixed (by the tensor component of the hyperfine interactions) with respect to the $SU(6)$ eigenstates of Figure 3. This mixing angle is predicted⁴ to be -32° , to be compared to a global fit to the data which gives $\theta_S \simeq -32^\circ$. (In contrast, the two $N^* \frac{3}{2}^-$ states are predicted to be weakly mixed with a mixing angle of only $+6^\circ$, versus the data which gives $\theta_D \simeq +10^\circ$). An immediate consequence of the $N^* \frac{1}{2}^-$ mixing is an explanation of the striking fact that the lower state, the $N^*(1535) \frac{1}{2}^-$, is very strongly coupled to $N\eta$ relative to $N\pi$ (even though phase space strongly favors the latter mode). The Table also illustrates that, at least in its current realizations, the constituent quark model is only a qualitative tool. Note in particular the four photocouplings: in typical fashion, the signs and general magnitudes of the amplitudes are satisfactory, but quantitative agreement is lacking. This point is elaborated in Table 2, which displays the predicted and observed photocouplings of the four-star (*i.e.*, well-established) N^* and Δ^* resonances. While once again lacking quantitative precision, most of these predictions depend critically on there being three active spin-1/2 degrees of

Table 1: Decay Amplitudes of $N^*(1535) \frac{1}{2}^-$ and $N^*(1650) \frac{1}{2}^-$

state	$N\pi$	$N\eta$	ΛK	$\Delta\pi$	γp	γn
$N^*(1535)$						
expt.	8 ± 3	$+8 \pm 4$	no	0 ± 2	$+68 \pm 10$	-59 ± 22
theory	5	+5	no	-2	+147	-119
$N^*(1650)$						
expt.	10 ± 2	-1 ± 1	-3 ± 1	-4 ± 1	$+52 \pm 17$	-11 ± 28
theory	9	-2	-3	-8	+88	-35

freedom in this system and on the spin of these degrees of freedom being fully engaged in transition amplitudes. Successes like these strongly suggest that this baby has great potential - - - even where spin is concerned - - - and that it should be nurtured along to maturity rather than abandoned!

2.3 Heavy Quarks Versus Light Quarks: A Curious Coincidence

In trying to understand the surprising successes of the constituent quark model, I have found it useful to compare light quark and heavy quark physics. Heavy Quark Symmetry⁶ rigorously defines the behavior of systems containing a single heavy quark Q as a function of $1/m_Q$. This behavior is observed in the \bar{B} and D meson systems, where it is supposed to work, but it also seems to work *qualitatively* as $m_Q \rightarrow m_d$, the light quark constituent mass. See Figure 6. This behavior is observed in more than just spectroscopy. For example, the amplitudes for $K_2^*(1420) \rightarrow K\pi$ and for $D_2^*(2640) \rightarrow D\pi$ are equal within errors, as they would be predicted to be⁶ if c and s were both heavy quarks. This picture strongly suggests to me that the degrees of freedom and the dynamics are the same all the way down the sequence $Q \rightarrow b \rightarrow c \rightarrow s \rightarrow u$ or d . Since in a heavy quark system this degree of freedom is specified by Heavy Quark Symmetry to be a simple spin-1/2 degree of freedom, this *data* seems to be telling us once again that the constituent quark model is on the right track.

Heavy Quark Symmetry applies to a pristine heavy quark moving in the fields of a "brown muck" of light quarks and glue. However, if a heavy quark remains pristine down to light quark masses, then the brown muck must also behave like a heavy quark. In other words, $Q\bar{Q}$ physics should also extrapolate down to light quark mass scales. Figure 7 shows that this also indeed seems to be the case all the way down to the pion!

Table 2: Photoproduction Amplitudes of Four Star Resonances

state	$A^p_{\frac{3}{2}}$	$A^p_{\frac{1}{2}}$	$A^n_{\frac{3}{2}}$	$A^n_{\frac{1}{2}}$
$\Delta(1232)_{\frac{3}{2}}^+$	-257 ± 8 -179	-141 ± 5 -103		
$N(1675)_{\frac{5}{2}}^-$	$+18 \pm 9$ $+16$	$+18 \pm 10$ $+12$	-70 ± 6 -53	-50 ± 14 -37
$N(1520)_{\frac{3}{2}}^-$	$+163 \pm 7$ $+128$	-22 ± 8 -23	-137 ± 13 -122	-62 ± 6 -45
$N(1535)_{\frac{1}{2}}^-$		$+68 \pm 10$ $+147$		-59 ± 22 -119
$N(1650)_{\frac{1}{2}}^-$		$+52 \pm 17$ $+88$		-11 ± 28 -35
$\Delta(1700)_{\frac{3}{2}}^-$	$+91 \pm 29$ $+105$	$+114 \pm 13$ $+100$		
$\Delta(1620)_{\frac{1}{2}}^-$		$+30 \pm 14$ $+59$		
$N(1680)_{\frac{5}{2}}^+$	$+135 \pm 17$ $+91$	-14 ± 8 ~ 0	-35 ± 11 -25	$+27 \pm 10$ $+26$
$N(1720)_{\frac{3}{2}}^+$	-26 ± 10 $+46$	$+27 \pm 24$ -133	-33 ± 59 -10	$+18 \pm 29$ $+57$
$N(1440)_{\frac{1}{2}}^+$		-72 ± 29 -24		$+52 \pm 25$ $+16$
$\Delta(1950)_{\frac{7}{2}}^+$	-101 ± 14 -69	-85 ± 17 -50		
$\Delta(1905)_{\frac{5}{2}}^+$	-31 ± 30 -33	$+37 \pm 16$ $+8$		
$\Delta(1910)_{\frac{1}{2}}^+$		$+13 \pm 22$ ~ 0		

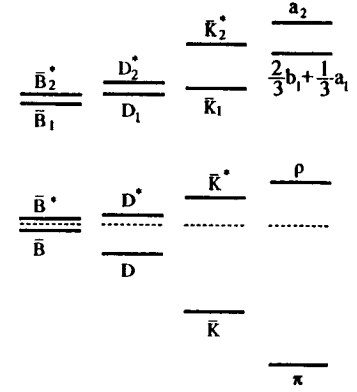


Figure 6: The evolution of "heavy-light" spectra from the \bar{B} to the π .

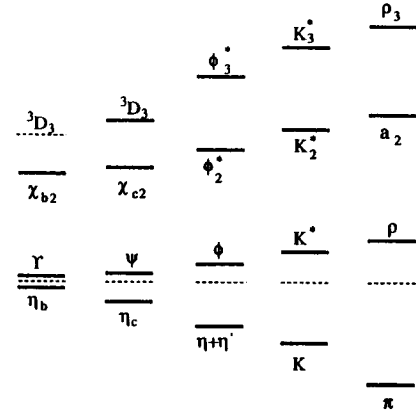


Figure 7: The evolution of "heavy-heavy" spectra from the Υ to the π .

3 Valence Spin Structure: A Pedestrian View

3.1 Introduction: The Proton's Spin in the Naïve Nonrelativistic Quark Model

In the naïve nonrelativistic quark model, the wavefunctions for a proton, a neutron, and a sigma-minus polarized along $+\hat{z}$ are

$$p_{\uparrow} = C_A u u d \sqrt{\frac{1}{6}} (\uparrow\uparrow\uparrow + \uparrow\uparrow\downarrow - 2 \uparrow\downarrow\downarrow) \psi(x_1, x_2, x_3) \quad (1)$$

$$n_{\uparrow} = C_A d d u \sqrt{\frac{1}{6}} (\uparrow\uparrow\uparrow + \uparrow\uparrow\downarrow - 2 \uparrow\downarrow\downarrow) \psi(x_1, x_2, x_3) \quad (2)$$

$$\Sigma_{\uparrow}^{-} = C_A d d s \sqrt{\frac{1}{6}} (\uparrow\uparrow\uparrow + \uparrow\uparrow\downarrow - 2 \uparrow\downarrow\downarrow) \psi(x_1, x_2, x_3) \quad (3)$$

in the SU(3) limit. Here ψ is the totally symmetric ground state spatial wavefunction that these particles have in common if $m_u = m_d = m_s$, the spin wavefunction $\sqrt{\frac{1}{6}}(\uparrow\uparrow\uparrow + \uparrow\uparrow\downarrow - 2 \uparrow\downarrow\downarrow)$ is the unique spin-1/2 combination symmetric in the exchange of the first two identical quarks, and C_A is the totally antisymmetric color state of the quarks. (We will need three states for the following analysis, and these three are particularly convenient because they have exactly two identical quarks in them.)

Let's now define q_{\uparrow} and q_{\downarrow} to be the probabilities of finding spin-up and spin-down quarks of type q in p_{\uparrow} , the polarized proton of Eqn. (1). Then in this naïve model one easily sees that

$$u_{\uparrow} = 5/3 \quad u_{\downarrow} = 1/3 \quad (4)$$

$$d_{\uparrow} = 1/3 \quad d_{\downarrow} = 2/3 \quad (5)$$

$$s_{\uparrow} = 0 \quad s_{\downarrow} = 0. \quad (6)$$

Given the successes of the naïve nonrelativistic quark model discussed above, we would expect these predictions to be roughly correct, and it is accordingly important to check them. *The interest and excitement surrounding the original EMC measurements⁷ of the polarized structure functions of the proton arose from their apparent conflict with these predictions.*

How do we go about measuring the probabilities q_{\uparrow} and q_{\downarrow} ? One way is to relate them to axial vector coupling constants. Consider the axial coupling constant in ordinary neutron β -decay:

$$G_A \equiv \langle p_{\uparrow} | A_{\uparrow}^z | n_{\uparrow} \rangle \quad (7)$$

where A_{\uparrow}^z is the \hat{z} -component of the ordinary (isospin-raising) axial vector current ($\bar{u}\gamma^z\gamma_5 d$ in terms of quark fields) and p_{\uparrow} and n_{\uparrow} are the states (1) and (2) at rest. Using the isospin ladder operators,

$$I_{-} | p_{\uparrow} \rangle = | n_{\uparrow} \rangle \quad (8)$$

so

$$G_A = \langle p_{\uparrow} | A_{\uparrow}^z I_{-} | p_{\uparrow} \rangle = \langle p_{\uparrow} | [A_{\uparrow}^z, I_{-}] | p_{\uparrow} \rangle \quad (9)$$

since $\langle p_{\uparrow} | I_{-} = 0$. Since A_{\uparrow}^z is the $+$ component of a vector operator under isospin,

$$[A_{\uparrow}^z, I_{-}] = 2A_3^z = \bar{u}\gamma^z\gamma_5 u - \bar{d}\gamma^z\gamma_5 d, \quad (10)$$

so

$$G_A = \langle p_{\uparrow} | \bar{u}\gamma^z\gamma_5 u - \bar{d}\gamma^z\gamma_5 d | p_{\uparrow} \rangle \quad (11)$$

and we have (in a model-independent way) re-expressed G_A in terms of expectation values of a flavor diagonal operator in the polarized proton. For a nonrelativistic quark

$$\bar{u}_s \gamma^z \gamma_5 u_s \simeq \chi_s^\dagger \sigma^z \chi_s, \quad (12)$$

where χ_s is a Pauli spinor, so

$$G_A \simeq \langle p_{\uparrow} | \sigma_u^z - \sigma_d^z | p_{\uparrow} \rangle = (u_{\uparrow} - u_{\downarrow}) - (d_{\uparrow} - d_{\downarrow}) = \Delta u - \Delta d \quad (13)$$

where we have defined

$$\Delta q \equiv q_{\uparrow} - q_{\downarrow}. \quad (14)$$

Eqn. (13), derived here using the nonrelativistic quark model, is actually more general, as we will see below. If we now use Eqns. (4-6), which are specific to the nonrelativistic quark model, we arrive at the usual result

$$G_A|_{nr} = \frac{5}{3} \quad (\text{experiment} : 1.26 \pm 0.01). \quad (15)$$

Next consider

$$G_A^{n\Sigma} \equiv \langle n_{\uparrow} | A_{\Delta S=1}^z | \Sigma_{\uparrow}^{-} \rangle \quad (16)$$

where $A_{\Delta S=1}^z = \bar{u}\gamma^z\gamma_5 s$ is the strangeness-changing axial vector current. This current is exactly analogous to $\bar{u}\gamma^z\gamma_5 d$: in the SU(3) limit there is a new symmetry called V -spin which is exactly analogous to I -spin which rotates $u \leftrightarrow s$ instead of $u \leftrightarrow d$. Thus

$$V_{-} | n_{\uparrow} \rangle = | \Sigma_{\uparrow}^{-} \rangle \quad (17)$$

can be compared to Eqn. (8). Moreover, continuing the correspondence gives

$$G_A^{n\Sigma} = \langle n_\uparrow | A_{\Delta S=1}^z V_- | n_\uparrow \rangle \quad (18)$$

$$= \langle n_\uparrow | [A_{\Delta S=1}^z, V_-] | n_\uparrow \rangle \quad (19)$$

$$= \langle n_\uparrow | \bar{u} \gamma^z \gamma_5 u - \bar{s} \gamma^z \gamma_5 s | n_\uparrow \rangle \quad (20)$$

as in Eqns. (9) to (11). If we now perform an ordinary isospin rotation of the right hand side of (20), we obtain

$$G_A^{n\Sigma} = \langle p_\uparrow | \bar{d} \gamma^z \gamma_5 d - \bar{s} \gamma^z \gamma_5 s | p_\uparrow \rangle \quad (21)$$

which once again expresses an axial vector coupling constant in terms of an expectation value of an operator in the proton. Using Eqn. (12) gives

$$G_A^{n\Sigma} = (d_\uparrow - d_\downarrow) - (s_\uparrow - s_\downarrow) = \Delta d - \Delta s, \quad (22)$$

which now depends on SU(2) and SU(3) symmetry. With Eqns. (4)-(6) we then obtain

$$G_A^{n\Sigma}|_{nr} = -\frac{1}{3} \quad (\text{experiment} : = -0.34 \pm 0.04). \quad (23)$$

The two results (15) and (23) seem consistent with the accuracy we expect from the nonrelativistic quark model, and suggest that the probabilities in Eqns. (4)-(6) are at least qualitatively correct. This is one reason the experimental results, to be introduced below, are so surprising. Before getting to this comparison, however, we will develop two more pieces of background.

3.2 Introduction: The Less Naïve Quark Model

The results derived so far depend not only on the wavefunctions (1)-(3), but also on the nonrelativistic approximation (12). In the real p, n , and Σ^- , the quark momenta are not small. As a result, the quark spinors have significant lower components:

$$u(\vec{p}s) \sim \begin{pmatrix} \chi_s \\ \frac{\vec{\sigma} \cdot \vec{p}}{E+m} \chi_s \end{pmatrix} \quad (24)$$

and as a result

$$\bar{u} \gamma^z \gamma_5 u = u^\dagger \gamma^0 \gamma^z \gamma_5 u \quad (25)$$

$$= u^\dagger \Sigma^z u \quad (26)$$

$$= (1 - \delta) \chi_s^\dagger \sigma^z \chi_s, \quad (27)$$

where $(1 - \delta)$ is a relativistic correction to (12) due to the presence of the lower components in (24) (in models, the expectation value of δ tends to be $\sim \frac{1}{4}$). These relations tell us that some of the "spin" of the quarks in a proton is in the orbital angular momentum of lower components. Such corrections mean that the *magnitude* of the Δq 's are smaller than predicted by Eqns. (4)-(6), i.e., that relativistic corrections will reduce in magnitude the naïve predictions (15) and (23).

There are other corrections to the results (15) and (23) even in the SU(3) limit. One is that the wavefunctions (1)-(3) are not the most general. Hyperfine interactions (which are certainly strong in this system: the $\Delta - N$ splitting is sizeable compared to orbital splittings) can perturb these wavefunctions by mixing into them a component with a mixed symmetry spatial wavefunction. Such components have probabilities for q_\uparrow and q_\downarrow which differ from the symmetric state. Many other corrections to these results are expected from SU(3) symmetry breaking and other sources, but model studies indicate that none of these effects apart from the relativistic correction δ have a major effect on the probabilities (4)-(6). In other words, should these probabilities prove to be very wrong, it will not be a failure that will be simple to accommodate within the context of the valence quark model.

3.3 Introduction: The Naïve Quark-Parton Model

If we view our hadrons in an infinite momentum frame (IMF: boost to $\mathbf{P} \rightarrow \infty$ along \hat{z}), then m_q and transverse momenta can be ignored. In this case

$$\bar{u} \gamma^z \gamma_5 u = \chi_s^\dagger \sigma^z \chi_s \quad (28)$$

as in the naïve nonrelativistic quark model, Eqn. (12). Moreover, we expect the quarks to be distributed in $x = p_{quark}^z / P$ with spin-dependent quark distribution functions $q_\uparrow(x)$ and $q_\downarrow(x)$ representing the probabilities of finding quarks with spin component $\pm \frac{1}{2}$ along \hat{z} and momentum fraction x . (In the general case we will also have antiquark and gluon spin-dependent distribution functions: see below). Since the relation (11) can be boosted to this frame, we now have

$$G_A = \int dx \{ [u_\uparrow(x) - u_\downarrow(x)] - [d_\uparrow(x) - d_\downarrow(x)] \} \quad (29)$$

$$\equiv \int dx \{ \Delta u(x) - \Delta d(x) \} \quad (30)$$

$$\equiv \Delta u - \Delta d, \quad (31)$$

where these Δq 's can be identified with those we had before only in the extreme nonrelativistic limit (where a boost is trivial), but where in general $\Delta q_{\text{IMF}} \neq \Delta q_{\text{rest}}$. We also have

$$G_A^{n\Sigma} = \Delta d - \Delta s \quad (32)$$

as before. If we had one more linearly independent measurement of the Δq 's, we could determine Δu , Δd , and Δs separately and thereby conclusively test the naïve predictions (4)-(6).

3.4 EMC: Enter Stage Right Minus Left

The EMC measurements⁷ of polarized lepton-polarized proton scattering provided the new linear combination of Δq 's that was needed to test the naïve quark model. In the lepton-quark center of mass frame at high energies

$$\frac{d\sigma}{d\Omega_{\text{cm}}} (\Rightarrow \Leftarrow) \propto e_q^2 \quad (33)$$

$$\frac{d\sigma}{d\Omega_{\text{cm}}} (\Rightarrow \Rightarrow) \propto e_q^2 \cos^2 \theta, \quad (34)$$

since, once $E \gg m$, helicity is conserved. As a result the cross sections in these reactions are in the ratio of 3:1 and

$$\sigma(\Rightarrow \Leftarrow) \propto \frac{4}{9}[u_\uparrow + \frac{1}{3}u_\downarrow] + \frac{1}{9}[d_\uparrow + \frac{1}{3}d_\downarrow] + \frac{1}{9}[s_\uparrow + \frac{1}{3}s_\downarrow] \quad (35)$$

$$\sigma(\Rightarrow \Rightarrow) \propto \frac{4}{9}[u_\uparrow + \frac{1}{3}u_\downarrow] + \frac{1}{9}[d_\uparrow + \frac{1}{3}d_\downarrow] + \frac{1}{9}[s_\uparrow + \frac{1}{3}s_\downarrow]. \quad (36)$$

If we define

$$q(x) \equiv q_\uparrow(x) + q_\downarrow(x) \quad (37)$$

then

$$A^p(x) \equiv \frac{\sigma(\Rightarrow \Leftarrow) - \sigma(\Rightarrow \Rightarrow)}{\frac{1}{2}[\sigma(\Rightarrow \Leftarrow) + \sigma(\Leftarrow \Leftarrow)]} = \frac{4\Delta u(x) + \Delta d(x) + \Delta s(x)}{4u(x) + d(x) + s(x)} \quad (38)$$

should be the polarization asymmetry for deep inelastic scattering at Bjorken variable x .

What would we expect to see? The naïve nonrelativistic quark model would say that the identical rest frame momentum distribution of the quarks in the wavefunctions (1)-(3) would lead to the x -dependent versions of Eqns. (4-6)

$$u_\uparrow(x) = 5v(x)/3 \quad u_\downarrow(x) = v(x)/3 \quad (39)$$

$$d_\uparrow(x) = v(x)/3 \quad d_\downarrow(x) = 2v(x)/3 \quad (40)$$

$$s_\uparrow(x) = 0 \quad s_\downarrow(x) = 0 \quad (41)$$

where $v(x)$ is a universal valence quark distribution function with $\int dx v(x) = 1$. Therefore, in this model

$$A^p(x)|_{nr} = \frac{1}{3}G_A \simeq 0.42, \quad (42)$$

independent of x . However, we know that this ultra-naïve model of the quark distribution function is not quite right. In the first place, there is a 'sea' of quark-antiquark pairs. However, a symmetric sea of pairs (*i.e.*, one contributing equal probabilities to $q_\uparrow(x)$, $q_\downarrow(x)$, $\bar{q}_\uparrow(x)$, and $\bar{q}_\downarrow(x)$ for all q) would not change Eqn. (42) since such a sea would give zero contribution to any Δq . A more relevant flaw of the ultra-naïve model is that as a result of its SU(6) symmetry it predicts that $u(x) = 2d(x)$ for all x . However, SU(6) is not a good symmetry and indeed the same forces that make $M_\Delta > M_N$ produce mixed symmetry components in the proton wave function (as mentioned in Section 3.2). Experimentally, such symmetry-breaking is observed. For example, in the absence of such effects, the neutron charge radius would be zero. However, more intimately related to our considerations is the direct observation in deep inelastic scattering that

$$\frac{d(x)}{u(x)} \sim (1-x) \quad \text{as } x \rightarrow 1. \quad (43)$$

If one builds this asymmetry into a 'not-so-naïve' quark model by taking the u and d spin-dependent structure functions to be proportional to the spin-independent ones (we also add a symmetric sea $\sigma(x)$ for completeness):

$$u_\uparrow(x) = 5u(x)/6 + \sigma(x) \quad u_\downarrow(x) = u(x)/6 + \sigma(x) \quad (44)$$

$$d_\uparrow(x) = d(x)/3 + \sigma(x) \quad d_\downarrow(x) = 2d(x)/3 + \sigma(x) \quad (45)$$

$$s_\uparrow(x) = s_\downarrow(x) = \bar{q}_\uparrow(x) = \bar{q}_\downarrow(x) = \sigma(x), \quad (46)$$

then one obtains the predictions⁸ of Fig. 8 for the polarized structure function

$$g_1(x) \equiv \frac{1}{2} \left[\frac{4}{9}\Delta u(x) + \frac{1}{9}\Delta d(x) + \frac{1}{9}\Delta s(x) \right] \quad (47)$$

obtained by using measured values for $u(x)$, $d(x)$, and $s(x)$ and Eqn. (38).

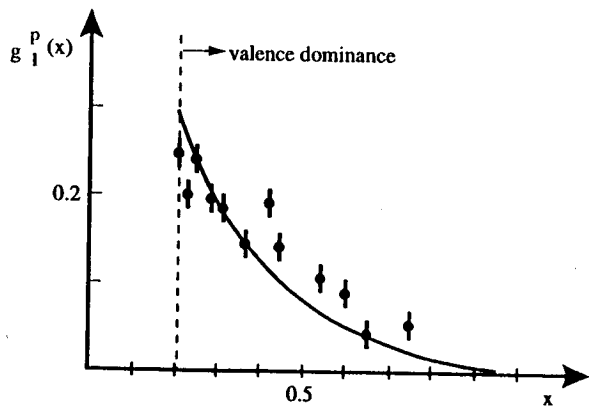


Figure 8: The 'not-so-naïve' quark model predictions for the proton spin-dependent structure function g_1^p versus the data.

3.5 Surprise

'Not-so-naïve' models seem to be able to predict G_A , $G_A^{n\Sigma}$, and g_1^p , so what's the problem? Fig. 8 shows only the valence quark region. When g_1^p is integrated over all x one gets

$$I^p \equiv \frac{1}{2} \left[\frac{4}{9} \Delta u + \frac{1}{9} \Delta d + \frac{1}{9} \Delta s \right] \simeq 0.14 \pm 0.01, \quad (48)$$

and it is here that the trouble starts. (I have updated the right hand side of Eqn. (48) to include some small perturbative corrections, as well as recent new data⁹).

If we had assumed that $\Delta s = 0$, then from G_A and $G_A^{n\Sigma}$ we would have deduced that $\Delta u = 0.92 \pm 0.04$ and $\Delta d = -0.34 \pm 0.04$ and would have predicted $I^p = 0.18$. This prediction (updated with new measurements) is that of the "Ellis-Jaffe sum rule"¹⁰, and it is in conflict with the measured value of I^p . Nevertheless, this accuracy still seems consistent with our expectations, so what's the problem? The "problem" arises when one solves the experimental equations (15), (23), and (48) for the Δq 's to obtain the results of Table 3. We see that even though the individual Δq 's are in reasonable agreement with

Table 3: The Δq 's and the total contribution S_q of quarks to the spin of the proton.

	experiment	nonrelativistic	relativistic ($\delta = 1/4$)
Δu	$0.78 \pm .06$	1.33	1.01
Δd	$-0.48 \pm .06$	-0.33	-0.25
Δs	$-0.14 \pm .06$	0.00	0.00
$2S_q$	$0.16 \pm .10$	1.00	0.75

naïve expectations, their sum, which measures twice the contribution of the quark spins to the spin of the proton, is much less than unity. Hence the problem: *what carries the spin of the proton and why does the quark model work as well as it does if the quarks are not responsible for the proton's spin?*

3.6 A Conservative Proposal: Unquenching the Quark Model

In the following, I will present arguments in support of a very conservative solution to the spin crisis: that the valence quarks have their expected "not-so-naïve" polarization $\Sigma_v \simeq 0.75$, but that sea quarks are polarized with $\Sigma_{sea} \simeq -0.15$ per flavor of light quark (see Figure 9). To make this case I will describe an explicit model in which the degrees of freedom of the flux tube model are expanded by allowing for the creation of $q\bar{q}$ loops ("unquenching"). Then I will describe the results of this model for Δs and for the strange electric and magnetic form factors of the proton, and speculate on an extension to $u\bar{u}$ and $d\bar{d}$ pairs which would resolve the "spin crisis".

A less conservative approach - - - which we consider premature before even attempting a rescue - - - is depicted in Figure 10.

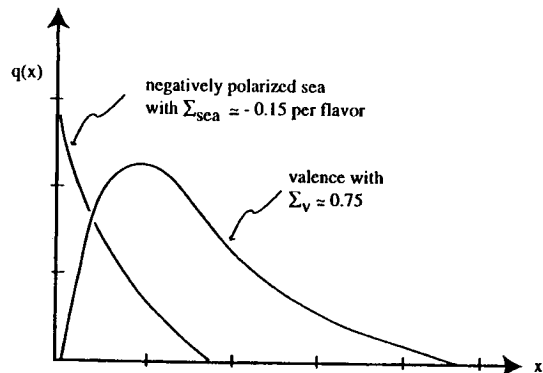


Figure 9: A schematic of the polarization of the valence and the sea quarks.



"Listen... You go tell Billy's mother, and I'll start looking for another old tree"

Figure 10: Models and QCD.

"The Far Side" by Gary Larson is reprinted courtesy Chronicle Features, San Francisco, California. All rights reserved.

4 Dressing the Baby

While it provides a good description of low-energy strong interaction phenomena, the constituent quark model appears to be inconsistent with many fundamental characteristics of QCD. Foremost among these inconsistencies is a "degree of freedom problem": the quark model declares that the low energy spectrum of QCD is built from the degrees of freedom of spin-1/2 fermions confined to a $q\bar{q}$ or qqq system. Thus, for mesons the quark model predicts - - - and we seem to observe - - - a "quarkonium" spectrum. In the baryons it predicts - - - and we seem to observe - - - the spectrum of two relative coordinates and three spin-1/2 degrees of freedom.

These quark model degrees of freedom are to be contrasted with the most naïve interpretation of QCD which would lead us to expect a low energy spectrum exhibiting 36 quark and antiquark degrees of freedom (3 flavors \times 2 spins \times 3 colors for particle and antiparticle), and 16 gluon degrees of freedom (2 spins \times 8 colors). Less naïve pictures exist, but none evade the first major "degree of freedom problem": the gluonic degrees of freedom appear to be missing from the low energy spectrum. This issue, being one of the most critical in Strong QCD, is being addressed by many theoretical and experimental programs.

The second major "degree of freedom problem" has to do with $q\bar{q}$ pair creation. *A priori*, one would expect pair creation to be so probable that a valence quark model would fail dramatically, while empirically pair creation is suppressed: the observed hadronic spectrum is dominated by narrow resonances, while the naïve picture would predict resonances with widths Γ comparable to their masses m .

We begin by dressing the naïve quark model with glue, although our main focus here will be on the effects of the $q\bar{q}$ sea.

4.1 Adiabatic Potentials and the Flux Tube Model

Consider first QCD without dynamical quarks in the presence of fixed $Q_1\bar{Q}_2$ or $Q_1Q_2Q_3$ sources¹¹. The ground state of QCD with these sources in place will be modified, as will be its excitation spectrum. For excitation energies below those required to produce a glueball, this spectrum will presumably be discrete for each value of the Q_1Q_2 relative spatial separation \vec{r} , with each eigenvalue being a continuous function of \vec{r} , as shown schematically in Fig. 11. There will be analogous spectra for $Q_1Q_2Q_3$ which are functions of the two relative coordinates $\vec{\rho} = \sqrt{1/2}(\vec{r}_1 - \vec{r}_2)$ and $\vec{\lambda} = \sqrt{1/6}(\vec{r}_1 + \vec{r}_2 - 2\vec{r}_3)$. We call the energy surface traced out by a given level of excitation as the positions of the sources are varied an adiabatic surface.

Let us now *define* the “quark model limit”: the quark model limit obtains when the quark sources move along the lowest adiabatic surface in such a way that they are isolated from the effects of other (excited) surfaces. We note that if this definition is relevant, it would have several appealing characteristics:

1) One of the great “mysteries” of the quark model is that it describes the mesons and baryons in terms of a wavefunction which only gives the amplitude for the valence quark variables, even though in QCD the general state vector must also refer to the glue fields. Indeed, in QCD for fixed Q_1 and Q_2 , for example, there are an infinite number of possible states of the glue so that it is certainly *not* sufficient to simply specify the state of the quarks. In the “quark model limit”, however, although there are an infinite number of possible glue states, for any fixed r there is one lowest-lying one. Moreover, although this lowest-lying state changes as r changes, it is completely determined by the quark coordinates. Thus we see the possibility that the quark model wavefunction had a “secret suppressed subscript” describing the state of the glue: $\psi_0(\vec{r})$. We will argue below that there should be analogous (but as yet undiscovered) worlds $\psi_n(\vec{r})$ for $n > 0$ corresponding to hybrid mesons.

2) The “quark model limit” can easily be seen to be inapplicable to any systems more complicated than $Q_1\bar{Q}_2$ and $Q_1Q_2Q_3$: such systems will always have adiabatic surfaces which cross so that the condition of isolation cannot be satisfied. It is thus not too surprising that $Q_1\bar{Q}_2$ and $Q_1Q_2Q_3$ may have a special status in QCD: only in these two cases is it possible that the state of the glue is (approximately) determined by the quark coordinates.

Before proceeding, we recall a simple molecular physics analogy to this proposed approximation. Diatomic molecular spectra can be described in an adiabatic approximation by holding the two relevant atomic nuclei at fixed separation r and then solving the Schrödinger problem for the (mutually interacting) electrons moving in the static electric field of the nuclei. The electrons will, for fixed r , have a ground state and excited states which will eventually become a continuum above energies required to ionize the molecule. The resulting adiabatic energy functions (when added to the internuclear Coulomb energy) then serve as effective internuclear potentials on which vibration-rotation spectra can be built. Molecular transitions can then take place within states built on a given surface or between surfaces.

In the “quark model limit” the quark sources play the rôle of the nuclei, and the glue plays the rôle of the electrons. From this point of view we can see clearly that conventional meson and baryon spectroscopy has only scratched

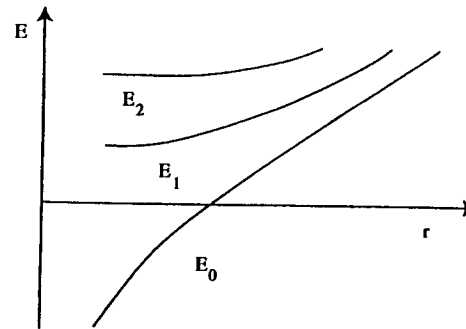


Figure 11: Schematic of the low-lying adiabatic surfaces of $Q_1\bar{Q}_2$ at separation r ; $E_0(r)$ is the gluonic ground state, $E_1(r)$ the first excited state, etc.

the surface of even $q_1\bar{q}_2$ and $q_1q_2q_3$ spectroscopy: so far we have only studied the vibration-rotation bands built on the lowest adiabatic surface corresponding to the gluonic ground state. We should expect to be able to build other “hadronic worlds” on the surfaces associated with excited gluonic states¹¹.

Note that the adiabatic approximation *certainly* applies in the limit of heavy quarks. Given the empirical evidence from Fig. 7, it seems that it must also apply to light quarks, even though this is somewhat surprising.

While the adiabatic approximation is more general, it is becoming increasingly firmly established that this approximation is realized in QCD in terms of the development of a confining chromoelectric flux tube. These flux tubes are the analog of the Abrikosov vortex lines that can develop in a superconductor subjected to a magnetic field, with the vacuum acting as a dual (*i.e.*, electric) superconductor creating a chromoelectric Meissner effect. A $Q\bar{Q}$ system held at fixed separation $r \gg \Lambda_{QCD}$ is known to have as its ground state a flux tube which leads to an effective low energy (adiabatic) potential corresponding to the standard “quarkonium” potential. However, this system also has excited states, corresponding to gluonic adiabatic surfaces in which a phonon has been excited in the flux tube, and on which spectra of “hybrid states” are built.

Lattice results allow us to check many aspects of the flux tube picture.



"Hoy! They're lighting their arrow... Can they do that?"

Figure 12: Theorist's tricks.

"The Far Side" by Gary Larson is reprinted courtesy Chronicle Features, San Francisco, California. All rights reserved.

For example, the lattice confirms the flux tube model prediction that sources with triality are confined with a string tension proportional to the square of their color Casimir. The predicted strongly collimated chromoelectric flux lines have also been seen on the lattice. I have found it particularly encouraging that the first excited adiabatic surfaces have been seen¹² with an energy gap $\delta V(r) = \pi/r$ above the quarkonium potential as predicted¹¹, and with the expected doubly-degenerate phonon quantum numbers. This strongly suggests that the J^{PC} exotic hybrid mesons predicted ten years ago¹¹ exist.

The flux tube model thus offers a possible explanation for one of the most puzzling apparent inconsistencies between the naïve quark model and QCD, although some of you may be asking yourselves the question posed in Fig. 12.

As will be discussed below, in the large N_c limit of QCD, hadrons do indeed consist of just their valence quarks and the glue between them. Thus the flux tube model may be viewed as a concrete realization of QCD in the large N_c limit.

4.2 Unquenching the Quark Model: Overview

There are three puzzles associated with the nature and importance of $q\bar{q}$ pairs in low energy hadron structure:

- 1) the origin of the apparent valence structure of hadrons (since even as $N_c \rightarrow \infty$, Z-graphs would produce pairs unless the quarks were heavy),
- 2) the apparent absence of unitarity corrections to naïve quark model spectroscopy, despite one's expectation of mass shifts $\Delta m \sim \Gamma$ (where Γ is a typical hadronic width), and
- 3) the systematic suppression of OZI-violating amplitudes A_{OZI} relative to one's expectation (from unitarity) that $A_{OZI} \sim \Gamma$.

In this section I will describe the solutions I see to these puzzles.

The Origin of the Valence Approximation

A weak form of the valence approximation seems to emerge from the large N_c limit² in the sense that diagrams in which only valence quark lines propagate through hadronic two-point functions dominate as $N_c \rightarrow \infty$. However, this dominance does not seem to correspond to the usual valence approximation since the Z-graph pieces of such diagrams will produce a $q\bar{q}$ sea.

Consider, however, the Dirac equation for a single light quark interacting with a static color source (or a single light quark confined in a bag). This equation represents the sum of a set of Feynman graphs which also include Z-graphs, but the effects of those graphs is captured in the lower components of the single-particle Dirac spinor. *I.e.*, such Z-graphs correspond to relativistic corrections to the quark model. That such corrections are important in the quark model has been known for a long time¹³. For us the important point is that while they have quantitative effects on quark model predictions (see, *e.g.*, Eqn. (27)), they do not qualitatively change the single-particle nature of the spectrum of the quark of our example, nor would they qualitatively change the spectrum of $q\bar{q}$ or qqq systems. Note that this interpretation is consistent with the fact that Z-graph-induced $q\bar{q}$ pairs do *not* correspond to the usual partonic definition of the $q\bar{q}$ sea since Z-graphs vanish in the infinite momentum frame. Thus the $q\bar{q}$ sea of the parton model is also associated with the $q\bar{q}$ loops of unquenched QCD.

The $\Delta m \ll \Gamma$ Problem

Consider two resonances which are separated by a mass gap δm in the narrow resonance approximation. In general we would expect that departures from the narrow resonance approximation, which produce resonance widths Γ , ought also to produce mass shifts Δm of order Γ . Yet even though a typical hadronic mass spectrum is characterized by mass gaps δm of order 500 MeV, and typical hadronic widths are of order 250 MeV, this does not seem to happen.

A simple resolution of this puzzle has been proposed¹⁴. As discussed in Section 4.1, in the flux tube model¹¹, the quark potential model arises from an adiabatic approximation to the gluonic degrees of freedom embodied in the flux tube. At short distances where perturbation theory applies, the effect of N_f types of light $q\bar{q}$ pairs is (in lowest order) to shift the coefficient of the Coulombic potential from $\alpha_s^{(0)}(Q^2) = \frac{12\pi}{33m(Q^2/\Lambda_3^2)}$ to $\alpha_s^{(N_f)}(Q^2) = \frac{12\pi}{(33-2N_f)m(Q^2/\Lambda_{N_f}^2)}$.

The net effect of such pairs is thus to produce a new effective short distance $Q\bar{Q}$ potential. Similarly, when pairs bubble up in the flux tube (*i.e.*, when the flux tube breaks to create a $Q\bar{q}$ plus $q\bar{Q}$ system and then "heals" back to $Q\bar{Q}$), their net effect is to cause a shift $\Delta E_{N_f}(\tau)$ in the ground state gluonic energy which in turn produces a new long-range effective $Q\bar{Q}$ potential¹⁵.

It has indeed been shown¹⁴ that the net long-distance effect of the bubbles is to create a new string tension b_{N_f} (*i.e.*, that the potential remains linear). Since this string tension is to be associated with the observed string tension, after renormalization pair creation has no effect on the long-distance structure of the quark model in the adiabatic approximation. Thus the net effect of mass shifts from pair creation is much smaller than one would naively expect from the typical width Γ : such shifts can only arise from nonadiabatic effects. For heavy quarkonium, these shifts can in turn be associated with states which are strongly coupled to nearby thresholds.

It should be emphasized that it was necessary to sum over very large towers of $Q\bar{q}$ plus $q\bar{Q}$ intermediate states to see that the spectrum was only weakly perturbed (after unquenching and renormalization). In particular, no simple truncation of the set of meson loop graphs can reproduce such results.

The Survival of the OZI Rule

There is another puzzle of hadronic dynamics which is reminiscent of this one: the success of the OZI rule³. A generic OZI-violating amplitude A_{OZI} can also be shown to vanish like $1/N_c$. However, there are several unsatisfactory features of this "solution" to the OZI mixing problem¹⁶. Consider ω - ϕ mixing as an example. This mixing receives a contribution from the virtual hadronic

loop process $\omega \rightarrow K\bar{K} \rightarrow \phi$, both steps of which are OZI-allowed, and each of which scales with N_c like $\Gamma^{1/2} \sim N_c^{-1/2}$. The large N_c result that this OZI-violating amplitude behaves like N_c^{-1} is thus not peculiar to large N_c : it just arises from "unitarity" in the sense that the real and imaginary parts of a generic hadronic loop diagram will have the same dependence on N_c . The usual interpretation of the OZI rule in this case - - - that "double hairpin graphs" are dramatically suppressed - - - is untenable in the light of these OZI-allowed loop diagrams. They expose the deficiency of the large N_c argument since $A_{OZI} \sim \Gamma$ is not a good representation of the OZI rule. (Continuing to use ω - ϕ mixing as an example, we note that $m_\omega - m_\phi$ is numerically comparable to a typical hadronic width, so the large N_c result would predict an ω - ϕ mixing angle of order unity in contrast to the observed pattern of very weak mixing which implies that $A_{OZI} \ll \Gamma \ll m$.)

Unquenching the quark model thus endangers the naïve quark model's agreement with the OZI rule. It has been shown¹⁷ how this disaster is naturally averted in the flux tube model through a "miraculous" set of cancellations between mesonic loop diagrams consisting of apparently unrelated sets of mesons (*e.g.*, the $K\bar{K}$, $K\bar{K}^* + K^*\bar{K}$, and $K^*\bar{K}^*$ loops tend to strongly cancel against loops containing a K or K^* plus one of the four strange mesons of the $L = 1$ meson nonets).

Of course the "miracle" occurs for a good reason. In the flux tube model, where pair creation occurs in the 3P_0 state, the overlapping double hairpin graphs which correspond to OZI-violating loop diagrams (see Fig. 13), cannot contribute in a closure-plus-spectator approximation since the 0^{++} quantum numbers of the produced (or annihilated) pair do not match those of the initial and final state for any established nonet. In fact¹⁷ this approximation gives zero OZI violation in all but the (still obscure) 0^{++} nonet. In addition, corrections to the closure-plus-spectator approximation are small, so that the observed hierarchy $A_{OZI} \ll \Gamma$ is reproduced.

We emphasize once again that such cancellations require the summation of a very large set of meson loop diagrams with cancellations between what are apparently unrelated sets of intermediate states.

Some Comments

We believe the preceding discussion strongly suggests that models¹⁸ which have not addressed the effects of unquenching on spectroscopy and the OZI rule should be viewed very skeptically as models of the effects of the $q\bar{q}$ sea on hadron structure: large towers of mesonic loops are required to understand how quarkonium spectroscopy and the OZI rule survive once strong pair creation

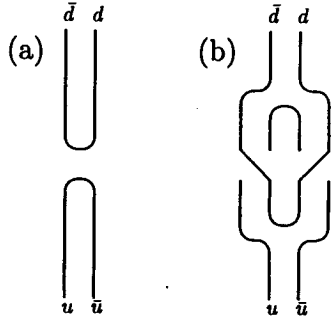


Figure 13: (a) OZI-violation in a meson propagator by "pure annihilation", corresponding to a disconnected double-hairpin diagram. (b) A different time ordering of the same Feynman graph gives an OZI-violating loop diagram via two OZI-allowed amplitudes.

is turned on. In particular, while pion and kaon loops (which tend to break the closure approximation due to their exceptional masses) have a special role to play, they cannot be expected to provide a reliable guide to the physics of $q\bar{q}$ pairs.

5 A Pair Creation Model for the Strangeness of the Proton

The following discussion of the strangeness content of the proton will be based on the quark-level process shown in Fig. 14(b). The main new feature of the calculation on which this discussion is based¹⁹ is a sum over a *complete set* of strange intermediate states, rather than just a few low-lying states. As explained above, this is *necessary* for consistency with the OZI rule and the success of quark model spectroscopy.

The lower vertex in Fig. 14(b) arises when $q\bar{q}$ pair creation perturbs the initial nucleon state vector so that, to leading order in pair creation,

$$|p\rangle \rightarrow |p\rangle + \sum_{Y^* K^* \ell S} \int q^2 dq |Y^* K^* q \ell S\rangle \frac{\langle Y^* K^* q \ell S | h_{q\bar{q}} | p\rangle}{M_p - E_{Y^*} - E_{K^*}}, \quad (49)$$

where $h_{q\bar{q}}$ is a quark pair creation operator, Y^* (K^*) is the intermediate baryon

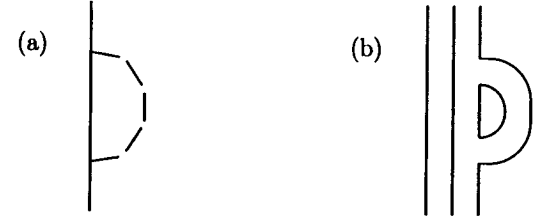


Figure 14: A meson loop correction to a baryon propagator, drawn at (a) the hadronic level, and (b) the quark level.

(meson), q and ℓ are the relative radial momentum and orbital angular momentum of Y^* and K^* , and S is the sum of their spins. Of particular interest is $s\bar{s}$ pair creation by the pair creation operator $h_{s\bar{s}}$, which will generate non-zero expectation values for strangeness observables:

$$\langle O_s \rangle = \sum_{\substack{Y^* K^* \ell S \\ Y^* K^* \ell S'}} \int q^2 dq q'^2 dq' \frac{\langle p | h_{s\bar{s}} | Y^* K^* q' \ell' S' \rangle}{M_p - E_{Y^*} - E_{K^*}} \times \langle Y^* K^* q' \ell' S' | O_s | Y^* K^* q \ell S \rangle \frac{\langle Y^* K^* q \ell S | h_{s\bar{s}} | p \rangle}{M_p - E_{Y^*} - E_{K^*}}. \quad (50)$$

The derivation of this simple equation, including the demonstration that it is gauge invariant, is straightforward¹⁹. We will be considering the cases $O_s = \Delta s$, R_s^2 , and μ_s , where Δs is as in Eqn. (14), and where R_s^2 and μ_s are the strangeness radius and magnetic moments to be defined more precisely below. The value of Δs can be associated (via small scale-dependent QCD radiative corrections) with the contribution of strange quarks to the deep inelastic spin-dependent structure functions and to the strange quark axial current matrix elements in the proton.

To calculate the $p \rightarrow Y^* K^*$ vertices in Eq. (49), the flux-tube-breaking model was used. This model, which reduces to the well-known 3P_0 decay model in a well-defined limit, had its origin in applications to decays of mesons^{20,21}

and baryons²². The model assumes that a meson or baryon decays when a chromoelectric flux tube breaks, creating a constituent quark and antiquark on the newly exposed flux tube ends. The pair creation operator is taken to have 3P_0 quantum numbers:

$$h_{q\bar{q}}(t, \mathbf{x}) = \gamma_0 \left(\frac{3}{8\pi r_q^2} \right)^{3/2} \int d^3z \exp\left(-\frac{3z^2}{8r_q^2}\right) q^\dagger\left(t, \mathbf{x} + \frac{\mathbf{z}}{2}\right) \alpha \cdot \nabla q\left(t, \mathbf{x} - \frac{\mathbf{z}}{2}\right). \quad (51)$$

The dimensionless constant γ_0 is the intrinsic pair creation strength, a parameter which we fit to the $\Delta \rightarrow N\pi$ width. The operator (51) creates *constituent* quarks, hence the pair creation point is smeared out by a gaussian factor whose width, r_q , is another parameter of the model. The parameter r_q is constrained by meson decay data to be approximately 0.25 fm^{14,17}.

Once an $s\bar{s}$ pair is created, the decay proceeds by quark rearrangement, as shown in Fig. 15. The $p \rightarrow Y^* K^*$ decay amplitude of the first of Figs. 15 may be written as

$$\langle Y^* K^* | h_{s\bar{s}} | p \rangle = \gamma_0 \bar{\Sigma} \cdot \bar{I}, \quad (52)$$

where $\bar{\Sigma}$ is a spin overlap which can be expressed in terms of the baryon and meson spin wavefunctions as

$$\bar{\Sigma} \equiv \sum_{s_1 \dots s_6} \chi_{s_1 s_2 s_3}^{*Y^*} \chi_{s_4 s_5}^{*K^*} \chi_{s_1 s_2 s_3}^p \bar{\chi}_{s_4 s_5}, \quad (53)$$

with

$$\bar{\chi}_{s_4 s_5} \equiv \begin{pmatrix} 2\delta_{s_4 1} \delta_{s_5 1} \\ -\delta_{s_4 1} \delta_{s_5 1} - \delta_{s_4 1} \delta_{s_5 1} \\ -2\delta_{s_4 1} \delta_{s_5 1} \end{pmatrix}, \quad (54)$$

and \bar{I} a spatial overlap:

$$\begin{aligned} \bar{I} &= 2\gamma_0 \left(\frac{3}{4\pi b} \right)^{3/2} \int d^3k d^3p d^3s \exp\left(\frac{-s^2}{2b}\right) \\ &\times \Phi_{Y^*}^* \left[\mathbf{k}, -\sqrt{\frac{3}{2}} \left(\mathbf{p} - \frac{\mathbf{s}}{2} - \frac{m_s}{m_{uu}} \mathbf{q} \right) \right] \Phi_{K^*}^* \left[\mathbf{p} + \frac{\mathbf{s}}{2} - \frac{m_s}{m_{us}} \mathbf{q} \right] \\ &\times p \exp\left(-\frac{2}{3} r_q^2 p^2\right) \Phi_p \left[\mathbf{k}, -\sqrt{\frac{3}{2}} \left(\mathbf{p} + \frac{\mathbf{s}}{6} - \mathbf{q} \right) \right]. \end{aligned} \quad (55)$$

Here the Φ 's are momentum space wavefunctions, \mathbf{q} is the momentum of Y^* , and the m_i 's are quark masses (m_{uu} is short for $2m_u + m_s$, etc.). The factor

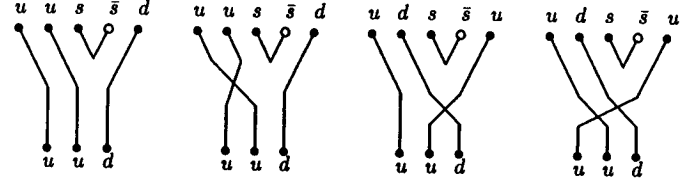


Figure 15: Quark line diagrams for $p \rightarrow \Sigma^* K^*$ and $p \rightarrow \Lambda^* K^*$.

$\exp(-s^2/2b)$ is the overlap of the initial and final-state flux tube wavefunctions; its size is controlled by the physical string tension b .

For the remaining quark line diagrams in Fig. 15, the decay amplitude still has the form (52), but the spin indices in Eq. (53) become permuted. The spatial overlap in (55) remains the same thanks to the assumed symmetry of the proton's spatial wavefunction.

Faced with the large number of states that contribute to the sum in Eq. (50), it was necessary to use simple harmonic oscillator (SHO) wavefunctions for the baryons and mesons in (55). The oscillator parameters β (defined by $\Phi(\mathbf{k}) \sim e^{-k^2/2\beta^2}$), were taken to be $\beta_{meson} = 0.4$ GeV for mesons²¹ and $\beta_{baryon} = 0.32$ GeV for baryons⁴. As discussed below, the results are quite insensitive to changes in the β 's (mainly because Eq. (50) is independent of the choice of wavefunctions in the closure limit - - any complete set gives the same result - - and the full calculation with energy denominators does not deviate much from this limit.)

Even with SHO wavefunctions, the sum over intermediate states would be very difficult were it not for an important selection rule: inspection of the quark line diagrams in Fig. 15 shows that the relative coordinate of the non-strange quarks in baryon Y^* is always in its ground state. Only the relative coordinate between the strange and non-strange quarks (i.e., the λ_{Y^*} -oscillator) can become excited. This drastically reduces the number of states that must be summed over. Unfortunately, this simplification does not apply for $u\bar{u}$ or $d\bar{d}$ pair creation.

It is useful to refer to the closure-spectator limit of Eq. (50). This is the limit in which the energy denominators do not depend strongly on the quantum numbers of Y^* and K^* , so that the sums over intermediate states collapse to 1, giving

$$\langle O_s \rangle \propto \langle p | h_{s\bar{s}} O_s h_{s\bar{s}} | p \rangle \propto \langle 0 | h_{s\bar{s}} O_s h_{s\bar{s}} | 0 \rangle, \quad (56)$$

where the second step follows since $h_{s\bar{s}}$ does not couple to the motion of the valence spectator quarks. We see that the expectation value of O_s is taken between the 3P_0 states created by $h_{s\bar{s}}$. From the J^{PC} of the 3P_0 pair it then follows that $\Delta s = R_s^2 = \mu_s = 0$ in the closure-spectator limit (a result which would not be seen if only the lowest term, or lowest few terms, were included in the closure sum).

In the next Section I will discuss the results for the expectation values defined by Eq. (50) for the quantities Δs , R_s^2 , and μ_s . We will see that delicate cancellations lead to small values for these observables even though the probability of $s\bar{s}$ pairs in the proton is substantial.

5.1 Strange Spin Content

Δs , the fraction of the proton's spin carried by strange quarks, is given by twice the expectation value of the s and \bar{s} spins :

$$\Delta s = 2 \langle S_z^{(s)} + S_z^{(\bar{s})} \rangle. \quad (57)$$

Let us first examine the contribution to Δs from just the lowest-lying intermediate state, ΛK . The P -wave ΛK state with $J = J_z = \frac{1}{2}$ is

$$|(\Lambda K)_{P\frac{1}{2}}\rangle = \sqrt{\frac{2}{3}} |(\Lambda_1 K)_{m=1}\rangle - \sqrt{\frac{1}{3}} |(\Lambda_1 K)_{m=0}\rangle. \quad (58)$$

The \bar{s} quark in the kaon is unpolarized, while the s quark in the Λ carries all of the Λ 's spin; because of the larger coefficient multiplying the first term in (58), the ΛK intermediate state alone gives a negative contribution to Δs .

When we add in the $(\Lambda K^*)_{P\frac{1}{2}}$ and $(\Lambda K^*)_{P\frac{3}{2}}$ states (note that the subscripts denote the quantities ℓS defined previously), we have

$$\Delta s \propto \begin{pmatrix} 1 & -\sqrt{\frac{1}{3}} & \sqrt{\frac{2}{3}} \end{pmatrix} \frac{1}{18} \begin{bmatrix} -3 & \sqrt{3} & -\sqrt{24} \\ & -1 & \sqrt{8} \\ & & 10 \end{bmatrix} \begin{pmatrix} 1 \\ -\sqrt{\frac{1}{3}} \\ \sqrt{\frac{2}{3}} \end{pmatrix} \quad (59)$$

in the closure limit. Here the matrix is just $2(S_z^{(s)} + S_z^{(\bar{s})})$ (which is of course symmetric), and the vectors give the relative coupling strengths of the proton to $[(\Lambda K)_{P\frac{1}{2}}, (\Lambda K^*)_{P\frac{1}{2}}, (\Lambda K^*)_{P\frac{3}{2}}]$. There are a couple of things to note here:

(1) The matrix multiplication in (59) evaluates to zero; there is no net contribution to Δs from the ΛK and ΛK^* states in the closure limit. There are in fact many such "sub-cancellations" in the closure sum for Δs : for each

fixed set of spatial quantum numbers in the intermediate state, the sum over quark spins alone gives zero (because $\langle S_z^{(s)} \rangle = \langle S_z^{(\bar{s})} \rangle = 0$ in the 3P_0 state). That is, each $SU(6)$ multiplet inserted into Eq. (50) separately sums to zero. Moreover, the Δs operator does not cause transitions between $I = 0$ and $I = 1$ strange baryons so that the Λ and Σ sectors are decoupled, hence they individually sum to zero.

(2) Only the diagonal term in Eq. (59) corresponding to $p \rightarrow (\Lambda K^*)_{P\frac{3}{2}} \xrightarrow{\Delta s} (\Lambda K^*)_{P\frac{3}{2}} \rightarrow p$ gives a positive contribution to Δs . (Here $\xrightarrow{\Delta s}$ denotes the action of the Δs operator.) All of the other terms give negative contributions. In the full calculation with energy denominators, the negative terms are enhanced because they contain kaon (rather than K^*) masses. The full calculation gives $\Delta s = -0.065$ from ΛK and ΛK^* states. The largest individual contribution is -0.086 , from the off-diagonal term $p \rightarrow (\Lambda K)_{P\frac{1}{2}} \xrightarrow{\Delta s} (\Lambda K^*)_{P\frac{3}{2}} \rightarrow p$.

For intermediate states containing Σ and Σ^* baryons, one finds

$$2(S_z^{(s)} + S_z^{(\bar{s})}) = \frac{1}{54} \begin{bmatrix} 3 & -12\sqrt{2} & 3\sqrt{3} & -6\sqrt{6} & 0 & 0 \\ & 15 & 0 & 0 & 6\sqrt{3} & -3\sqrt{15} \\ & & -7 & -10\sqrt{2} & -4\sqrt{2} & -4\sqrt{10} \\ & & & 10 & 4 & 4\sqrt{5} \\ & & & & -2 & -2\sqrt{5} \\ & & & & & 17 \end{bmatrix} \quad (60)$$

in the basis $[(\Sigma K)_{P\frac{1}{2}}, (\Sigma^* K)_{P\frac{1}{2}}, (\Sigma K^*)_{P\frac{1}{2}}, (\Sigma K^*)_{P\frac{3}{2}}, (\Sigma^* K^*)_{P\frac{1}{2}}, (\Sigma^* K^*)_{P\frac{3}{2}}]$. The corresponding relative couplings to the proton are $[-\frac{1}{3}, -\sqrt{\frac{8}{9}}, \sqrt{\frac{25}{27}}, \sqrt{\frac{8}{27}}, \sqrt{\frac{8}{27}}, \sqrt{\frac{40}{27}}]$.

Again, the net Δs from these states is zero in the closure limit, but this time the insertion of energy denominators does not spoil the cancellation very much: the full calculation gives $\Delta s = -0.003$ in this sector.

P -wave hyperons and kaons contribute another -0.04 to Δs , and the net contribution from all higher states is -0.025 . Thus, the result of the calculation¹⁹ is $\Delta s = -0.13$, in quite good agreement with the most recent extractions from experiment²³ $\Delta s = -0.10 \pm 0.03$. It should be emphasized that all parameters of this calculation were fixed by spectra and decay data. Moreover, the result is quite stable to parameter changes, varying by at most ± 0.025 when r_q , b , β_{baryon} and β_{meson} are individually varied by 30%.

For comparison with other calculations, note that the ΛK intermediate state alone contributes -0.030 to Δs , and the contribution from the ΛK , ΣK , and $\Sigma^* K$ states together is (coincidentally) also -0.030 .

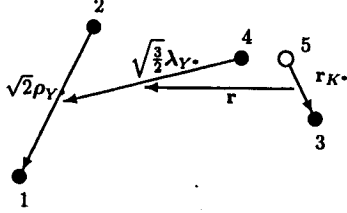


Figure 16: Quark coordinates in an intermediate state.

It is interesting to observe that Δs is driven mainly by meson, rather than baryon mass splittings: if one sets $m_\Lambda = m_\Sigma = m_{\Sigma^*}$, then Δs decreases by only about 30%, whereas it drops by about 80% if one sets $m_K = m_{K^*}$. Finally, an analogous calculation gives for the charm-quark contribution to the proton spin $\Delta c \approx -0.01$.

5.2 Strangeness Radius

Figure 16 defines our spatial variables for the quarks in an intermediate state. The (squared) distances of the s and \bar{s} quarks from the baryon-meson center of mass are

$$r_s^2 = (r_4 - \mathbf{R}_{cm})^2 = \left[-\sqrt{6} \left(\frac{m_u}{m_{uus}} \right) \lambda_{\gamma^*} + \epsilon_{K^*} \mathbf{r} \right]^2 \quad (61)$$

$$r_{\bar{s}}^2 = (r_6 - \mathbf{R}_{cm})^2 = \left[-\left(\frac{m_u}{m_{uus}} \right) r_{K^*} - \epsilon_{\gamma^*} \mathbf{r} \right]^2, \quad (62)$$

where $\epsilon_{K^*} \equiv M_{K^*}/M_{\gamma^*K^*}$ and $\epsilon_{\gamma^*} \equiv M_{\gamma^*}/M_{\gamma^*K^*}$, while by definition

$$R_s^2 \equiv r_s^2 - r_{\bar{s}}^2 \quad (63)$$

is the strangeness radius.

The calculation of R_s^2 is more difficult than the calculation of Δs , for several reasons. First, the operators appearing in R_s^2 cause orbital and radial transitions among the intermediate states. Thus SHO transitions satisfying

$\Delta n = 0, \pm 1$ and/or $\Delta \ell = 0, \pm 1$ are allowed, so there are many more terms to calculate (n and ℓ are orbital and radial SHO quantum numbers). Moreover, the sub-cancellations discussed above no longer occur, so that R_s^2 converges more slowly than Δs : more states must be included in Eq.(50) to obtain good accuracy. In addition, the basic matrix elements are more complicated: in a basis of states with good magnetic quantum numbers (m, m'), for example,

$$\begin{aligned} \langle n' \ell' m' | r_{K^*z} | n \ell m \rangle = & \\ \delta_{\ell' \ell-1} \delta_{m' m} \beta_{K^*} A_{\ell, m} \left(\sqrt{n + \ell + 1/2} \delta_{n' n} - \sqrt{n + 1} \delta_{n' n+1} \right) & \\ + \delta_{\ell' \ell+1} \delta_{m' m} \beta_{K^*} A_{\ell+1, m} \left(\sqrt{n + \ell + 3/2} \delta_{n' n} - \sqrt{n} \delta_{n' n-1} \right) & \quad (64) \end{aligned}$$

for matrix elements of the meson internal coordinate and

$$\begin{aligned} \langle q' \ell' m' | r_z | q \ell m \rangle = & i \delta_{m' m} \left\{ \delta_{\ell' \ell-1} A_{\ell, m} \left[-\frac{d}{dq} + \frac{\ell-1}{q} \right] \right. \\ & \left. - \delta_{\ell' \ell+1} A_{\ell+1, m} \left[\frac{d}{dq} + \frac{\ell+2}{q} \right] \right\} \frac{\delta(q-q')}{q^2} \quad (65) \end{aligned}$$

for matrix elements of the $Y^* - K^*$ relative coordinate, where we have defined $A_{\ell m} = \sqrt{\frac{(\ell+m)(\ell-m)}{(2\ell+1)(2\ell-1)}}$. These matrix elements must be coupled together to give $\langle R_s^2 \rangle$ between states of definite ℓ and S with total angular momentum $\frac{1}{2}$, leading to formulas which become quite lengthy, especially for excited intermediate states. There is fortunately a stringent check of the results: when one equates all of the energy denominators in Eq. (50), the closure-spectator result, $R_s^2 = 0$, must be obtained.

The results for R_s^2 are shown in Table 4. With the standard parameter set, $R_s^2 = -0.04 \text{fm}^2$. For reasonable parameter variations, R_s^2 ranges between -0.02 and -0.06fm^2 . Table 4 shows that the lowest-lying $SU(6)$ multiplets of intermediate states (i.e., the S -wave hyperons and kaons) account for about half of r_s^2 and $r_{\bar{s}}^2$. Most of the remaining contributions come from P -wave hyperons and kaons. However, R_s^2 involves a large cancellation between r_s^2 and $r_{\bar{s}}^2$, and its value doesn't settle down until we add in quite highly excited intermediate states. For this reason, the precise numerical value (and perhaps

Table 4: Proton strangeness radius from hadronic loops (in fm²). The rows give the running totals as progressively more excited intermediate states are added into the calculation. The final column thus shows the total from all intermediate states.

	S-waves	plus P-waves	plus D-waves and S-wave radial excitations	all states
r_s^2	.097	.198	.210	.173
$r_{\bar{s}}^2$.094	.139	.185	.210
R_s^2	.003	.059	.025	-.04

even the sign) of R_s^2 cannot be considered definitive: the conclusion is rather that R_s^2 is small, about an order of magnitude smaller than r_s^2 and $r_{\bar{s}}^2$. This result is not too surprising: R_s^2 is exactly zero in the closure limit, and previous hadronic loop studies^{14,17} led one to expect that the full calculation with energy denominators would preserve the qualitative features of this limit.

Note that the ΛK intermediate state alone gives $R_s^2 \approx -0.01\text{fm}^2$ (the sign is as expected from the usual folklore) while the ΛK , ΣK , and $\Sigma^* K$ states together give -0.017fm^2 . Nevertheless, although the sum over all states gives the same sign and order of magnitude as these truncations, Table 4 shows that this is just a coincidence.

5.9 Strange Magnetic Moment

The strange and antistrange quarks carry magnetic moments $-\frac{1}{3}\mu^{(s,\bar{s})}$ where

$$\mu^{(s)} = \frac{1}{2m_s} \langle 2S_z^{(s)} + L_z^{(s)} \rangle \quad (66)$$

$$\mu^{(\bar{s})} = -\frac{1}{2m_s} \langle 2S_z^{(\bar{s})} + L_z^{(\bar{s})} \rangle \quad (67)$$

and we denote the net strange magnetic moment by μ_s :

$$\mu_s \equiv \mu^{(s)} + \mu^{(\bar{s})}. \quad (68)$$

The spin expectation values are already in hand from the Δs calculation. Referring again to Fig. 16, we see that the s and \bar{s} orbital angular momenta are given by

$$\begin{aligned} L_s &= (\mathbf{r}_4 - \mathbf{R}_{cm}) \times \mathbf{p}_4 \\ &= \left[-\sqrt{6} \left(\frac{m_u}{m_{uus}} \right) \lambda_{Y^*} + \epsilon_{K^*} \cdot \mathbf{r} \right] \times \left[-\frac{2}{\sqrt{6}} \mathbf{p}_{\lambda_{Y^*}} + \left(\frac{m_s}{m_{uus}} \right) \mathbf{q} \right] \end{aligned} \quad (69)$$

$$\begin{aligned} L_{\bar{s}} &= (\mathbf{r}_5 - \mathbf{R}_{cm}) \times \mathbf{p}_5 \\ &= \left[-\left(\frac{m_u}{m_{us}} \right) \mathbf{r}_{K^*} - \epsilon_{Y^*} \cdot \mathbf{r} \right] \times \left[-\mathbf{p}_{K^*} - \left(\frac{m_s}{m_{us}} \right) \mathbf{q} \right]. \end{aligned} \quad (70)$$

Computing the expectation values of these operators presents no new difficulties beyond those encountered in the R_s^2 calculation. In fact, there are no radial transitions in this case, so there are fewer states to sum over and the sum converges more quickly.

The results obtained with the standard parameter set are

$$\begin{aligned} \langle 2S_z^{(s)} \rangle &= -0.058 & \langle 2S_z^{(\bar{s})} \rangle &= -0.074 \\ \langle L_z^{(s)} \rangle &= 0.043 & \langle L_z^{(\bar{s})} \rangle &= 0.038 \\ \mu^{(s)} &= -0.025\mu_N & \mu^{(\bar{s})} &= 0.060\mu_N \end{aligned} \quad (71)$$

$$\mu_s = 0.035\mu_N$$

The result is a positive (albeit small) value for μ_s , in disagreement with most other models. Where does the positive sign originate? First note that the signs of $\langle S_z^{(s)} \rangle$, $\langle L_z^{(s)} \rangle$, and $\langle L_z^{(\bar{s})} \rangle$ are correctly given by just the lowest lying intermediate state, ΛK of Eq. (58). (Note that the L_z 's have similar magnitudes so that orbital angular momentum contributes very little to μ_s in any case.) On the other hand, the ΛK state has $\langle S_z^{(\bar{s})} \rangle = 0$, whereas $\langle S_z^{(s)} \rangle$ is quite large and negative. (The main contribution comes from the off-diagonal process $p \rightarrow (\Lambda K)_{P\frac{1}{2}^+} \xrightarrow{S_z^{(s)}} (\Lambda K^*)_{P\frac{3}{2}^+} \rightarrow p$, although there is also a significant contribution from $p \rightarrow (\Lambda(1405)K)_{S\frac{1}{2}^+} \xrightarrow{S_z^{(s)}} (\Lambda(1405)K^*)_{S\frac{3}{2}^+} \rightarrow p$.) These important terms, which drive μ_s positive, are omitted in calculations which include only kaon loops. (The ΛK intermediate state alone contributes $-0.080\mu_N$ to μ_s , and the contribution from ΛK , ΣK , and $\Sigma^* K$ together is $-0.074\mu_N$.)

5.4 Comments on the Effects of $s\bar{s}$ Loops

The calculations just described here represent parameter-free calculations of the effects of the $s\bar{s}$ sea generated by strong $Y^* K^*$ loops on the low energy,

nonperturbative structure of the nucleons. They are to my knowledge the first such results within a framework which has been demonstrated to be consistent with the many empirical constraints which should be applied to such calculations, namely consistency with the success of the quark potential model's spectroscopy and especially with the validity of the OZI rule.

The results indicate that observable effects from the strange sea generated by such loops arise from delicate cancellations between large contributions involving a surprisingly massive tower of virtual meson-baryon intermediate states. If correct, these conclusions rule out the utility of a search for a simple but predictive low energy hadronic truncation of QCD. While complete (in the sense of summing over all OZI-allowed Y^*K^* loops) and gauge invariant, the calculation has ignored pure OZI-forbidden effects as well as certain loop diagrams directly generated by the probing current (independently gauge invariant contact terms). As a consequence, they cannot strictly speaking be taken as predictions for Δs , R_s^2 , or μ_s . Rather, the calculation shows that a complete set of strong Y^*K^* loops, computed in a model consistent with the OZI rule, gives very small observable $s\bar{s}$ effects. While such OZI-allowed processes *might* dominate, one cannot rule out the possibility (as was also the case with $\omega - \phi$ and other meson mixing¹⁷) that direct OZI violation (and in this case contact graphs as well) could make additional contributions of a comparable magnitude.

The small residual effect calculated for the loop contributions to Δs seems consistent with the most recent analyses of polarized deep inelastic scattering data. The calculations also give small residual strange quark contributions to the charge and magnetization distributions inside the nucleons. If these contributions are dominant, it will be a challenge to devise experiments that are capable of seeing them. Indeed, they are sufficiently small that their observation would appear to require the development of special apparatus dedicated to this task. Given the fundamental nature of the puzzling absence of other signals for the strong $q\bar{q}$ sea in low energy phenomena, this effort seems very worthwhile.

It would be desirable to devise tests of the mechanisms underlying the delicate cancellations which conspire to hide the effects of the sea in this picture. It also seems very worthwhile to extend such a calculation to $u\bar{u}$ and $d\bar{d}$ loops. Such an extension could reveal the origin of the observed violations²⁴ of the Gottfried Sum Rule²⁵ and also complete our understanding of the origin of the spin crisis. Since the effects of the $s\bar{s}$ loops are generally at high mass, it seems likely that the Pauli principle will have only a minor effect on $u\bar{u}$ and $d\bar{d}$ loops. Thus, from this calculation, I consider it likely that these lighter quarks will carry an even larger negative polarization than strange quarks,

making it plausible that the "missing spin" of the proton is in orbital angular momentum.

6 Summary

In these lectures I have advocated treating the phenomenology of QCD in two steps. In the zeroth order, Strong QCD is approximated by a relativistic constituent quark model with flux tube gluodynamics. As a second step, $q\bar{q}$ sea and other $1/N_c$ effects are added as perturbations.

We have seen here how the quark model might be "unquenched" in a way that preserves its spectroscopic successes and respects the OZI rule. All of the results presented are qualitative, but the model appears to be a viable candidate to explain the underlying physics.

If the picture I have advocated is correct, there are some immediate consequences:

1. Low energy hadronizations of QCD are in trouble, since sums over large towers of states were required to preserve the spectrum and the OZI rule,
2. $\Delta s \simeq -0.13$, suggesting $\Delta u \sim \Delta d \sim -0.2$, implies that when combined with $\Sigma_{valence} \sim 0.75$, the missing spin of the proton would reside in orbital angular momentum, and
3. μ_s and r_s^2 are small.

This discussion has also made it clear that "singlet physics" has revealed a serious flaw in the constituent quark model which had been hidden by minus signs:

$$\Delta u - \Delta d = (\Delta u_v + \Delta u_{sea}) - (\Delta d_v + \Delta d_{sea}) \simeq \Delta u_v - \Delta d_v, \quad (72)$$

so that non-singlet quantities like the Bjorken Sum Rule²⁶ are misleading about the success of the quenched quark model. However, it now seems plausible that the unquenched quark model can successfully describe those properties strongly affected by the sea, so I will close by declaring:

**THE QUARK MODEL IS DEAD
LONG LIVE THE QUARK MODEL.**

Acknowledgements

I would like to express my special thanks to Paul Geiger, with whom all of the new results described herein on the role of $q\bar{q}$ loops were obtained.

References

1. F.E. Close, private communication, cogently advocates using this term instead of the negative "nonperturbative QCD".
2. G. 't Hooft, Nucl. Phys. **B72**, 461 (1974); E. Witten, Nucl. Phys. **B160**, 57 (1979). For some recent very important developments in the $1/N_c$ expansion for baryons, see R. Dashen and A. Manohar, Phys. Lett. **B315**, 425 (1993); **B315**, 438 (1993); R. Dashen, E. Jenkins and A. Manohar, Phys. Rev. **D49**, 4713 (1994); **D51**, 2489 (1995).
3. S. Okubo, Phys. Lett. **5**, 165 (1963); Phys. Rev. **D 16**, 2336 (1977); G. Zweig, CERN Report No. 8419 TH 412, 1964 (unpublished); reprinted in *Developments in the Quark Theory of Hadrons*, edited by D. B. Lichtenberg and S. P. Rosen (Hadronic Press, Massachusetts, 1980); J. Iizuka, K. Okada, and O. Shito, Prog. Th. Phys. **35**, 1061 (1966); J. Iizuka, Prog. Th. Phys. Suppl. **37-38**, 21 (1966).
4. N. Isgur and G. Karl, Phys. Lett. **72B**, 109 (1977); **74B**, 353 (1978); Phys. Rev. **D 18**, 4187 (1978); **19**, 2653 (1979); L.A. Copley, N. Isgur, and G. Karl, *ibid.* **20**, 768 (1979); N. Isgur and G. Karl, *ibid.* **21**, 3175 (1980); and for a review see N. Isgur in *Modern Topics in Electron Scattering*, ed. B. Frois and I. Sick, (World Scientific, Singapore, 1991), p. 2.
5. R. Koniuk and N. Isgur, Phys. Rev. Lett. **44**, 485 (1980); Phys. Rev. **D 21**, 1868 (1980).
6. N. Isgur and M.B. Wise, Phys. Lett. **B237**, 527 (1990); **B232**, 113 (1989); Phys. Rev. Lett. **66**, 1130 (1991); and in *B Decays*, ed. S. Stone (World Scientific, Singapore, 1991), p. 158.
7. J. Ashman *et al.*, EMC Collaboration, Phys. Lett. **B206**, 364 (1988); Nucl. Phys. **B328**, 1 (1989).
8. F.E. Close and A.W. Thomas, Phys. Lett. **B212**, 227 (1988).
9. B. Adeva *et al.*, SMC Collaboration, Phys. Lett. **B302**, 533 (1993); P.L. Anthony *et al.*, E142 Collaboration, Phys. Rev. Lett. **71**, 959 (1993); D. Adams *et al.*, SMC Collaboration, Phys. Lett. **B329**, 399 (1994); K. Abe *et al.*, E143 Collaboration, SLAC preprint 6508 (1994), submitted to Physical Review Letters.

10. J. Ellis and R.L. Jaffe, Phys. Rev. **D9**, 1444 (1974); Phys. Rev. **D 10**, 1669 (1974).
11. N. Isgur and J. Paton, Phys. Rev. **D 31**, 2910 (1985).
12. See, e.g., S. Perantonis and C. Michaels, Nucl. Phys. **B347**, 854 (1990).
13. N.N. Bogoliubov, Ann. Inst. Henri Poincaré **8**, 163 (1968); A. LeYaouanc *et al.*, Phys. Rev. **D 9**, 2636 (1974); **15**, 844 (1977) and references therein; Michael J. Ruiz, *ibid.* **12**, 2922 (1975); A. Chodos, R.L. Jaffe, K. Johnson, and C.B. Thorn, *ibid.* **10**, 2599 (1974).
14. P. Geiger and N. Isgur, Phys. Rev. **D 41**, 1595 (1990).
15. Unlike the Coulombic region where the $q\bar{q}$ pairs are all virtual, in the long-distance region pair production can also lead to real dissociation into a $Q\bar{q}$ plus $q\bar{Q}$ system if the energy $E_0(r)$ corresponds exactly to the sum of the masses of states of these two meson subsystems. In the language of adiabatic surfaces, these dissociations occur when the $Q\bar{Q}$ adiabatic surface unperturbed by $q\bar{q}$ pair creation crosses the energies $E_{ij} = m_i^{Qq} + m_j^{qQ}$ corresponding to the two-meson adiabatic surfaces (which are independent of r for large r and have no continuum parts since the Q and \bar{Q} are fixed). The shifted adiabatic surface can, of course, be tracked through the level crossings to follow the quantum state that remains dominantly a $Q\bar{Q}$ pair connected by a flux tube.
16. H.J. Lipkin, Nucl. Phys. **B291**, 720 (1987); Phys. Lett. **B179**, 278 (1986); Nucl. Phys. **B244**, 147 (1984); Phys. Lett. **B124**, 509 (1983).
17. P. Geiger and N. Isgur, Phys. Rev. **D 44**, 799 (1991); Phys. Rev. Lett. **67**, 1066 (1991); Phys. Rev. **D 47**, 5050 (1993); P. Geiger, *ibid.* **49**, 6003 (1993).
18. R.L. Jaffe, Phys. Lett. **B229**, 275 (1989); G. Höhler *et al.*, Nucl. Phys. **B114**, 505 (1976); W. Koepf, E.M. Henley, and S.J. Pollock, Phys. Lett. **B288**, 11 (1992); M.J. Musolf and M. Burkardt, Z. Phys. **C 61**, 433 (1994); H. Ito, Phys. Rev. **C52**, R1750 (1995); B. Holzenkamp, K. Holinde, and J. Speth, Nucl. Phys. **A500**, 485 (1989); A. Szczurek and H. Holtmann, Acta Phys. Pol. **B 24**, 1833 (1993); H. Holtmann, A. Szczurek, and J. Speth, KFA-IKP(TH)-1994-25; T.D. Cohen, H. Forkel, and M. Nielsen, Phys. Lett. **B316**, 1 (1993); H. Forkel *et al.*, *Stranger in the light: the strange vector form factors of the nucleon*, UMPP #94-097 (hep-ph/9408326).
19. P. Geiger and N. Isgur, to appear in Phys. Rev. **D**.
20. L. Micu, Nucl. Phys. **B10**, 521 (1969); A. Le Yaouanc, L. Oliver, O. Pene, and J.-C. Raynal, Phys. Rev. **D 8**, 2233 (1973); Phys. Lett. **B71**, 397 (1977); *ibid.* **B72**, 57 (1977); W. Roberts and B. Silvestre-Brac, Few Body Syst. **11**, 171 (1992); P. Geiger and E.S. Swanson, Phys. Rev.

- D 50, 6855 (1994).
21. R. Kokoski and N. Isgur, Phys. Rev. D 35, 907 (1987);
 22. Fl. Stancu and P. Stassart, Phys. Rev. D 38, 233 (1988); 39, 343 (1989); 41, 916 (1990); 42, 1521 (1990); S. Capstick and W. Roberts, Phys. Rev. D 47, 1994, (1993); Phys. Rev. D 49, 4570, (1994).
 23. J. Ellis and M. Karliner, *Determination of α_s and the Nucleon Spin Decomposition using Recent Polarized Structure Function Data*, CERN-TH-7324/94, TAUP-2178-94 (hep-ph/9407287).
 24. P. Amaudruz *et al.*, New Muon Collaboration, Phys. Rev. Lett. 66, 2712 (1991); M. Arneodo *et al.*, Phys. Rev. D 50, R1, (1994); A. Baldit *et al.*, NA 51 Collaboration, Phys. Lett. B332, 244 (1994).
 25. K. Gottfried, Phys. Rev. Lett. 18, 1174 (1967). For some recent theoretical studies, see W.-Y. P. Hwang and J. Speth, Chin. Jour. Phys. 29, 461 (1991); A. Szczurek and J. Speth, Nucl. Phys. A 555, 249 (1993); V.R. Zoller, Z. Phys. C 53, 443 (1992); S. Kumano, Phys. Rev. D 43, 59 (1991); *ibid.*, 3067 (1991); S. Kumano and J. Londergan, Phys. Rev. D 44, 717(1991); E.M. Henley and G.A. Miller, Phys. Lett. B251, 453 (1990); A. Signal, A.W. Schreiber, and A.W. Thomas, Mod. Phys. Lett. A6, 271 (1991); W.-Y. P. Hwang, J. Speth, and G.E. Brown, Z. Phys. A 339, 383 (1991); and H. Holtmann, A. Szczurek, and J. Speth, KFA-IKP(TH)-1994-25.
 26. J.D. Bjorken, Phys. Rev. 148, 1467 (1966); Phys. Rev. D 1, 1376 (1970).